Journal of Power Sources 217 (2012) 268–279

Contents lists available at SciVerse ScienceDirect

Journal of Power Sources

journal homepage: www.elsevier.com/locate/jpowsour

Lattice Boltzmann simulation of liquid water transport in turning regions of serpentine gas channels in proton exchange membrane fuel cells

Bo Han, Hua Meng*

School of Aeronautics and Astronautics, Zhejiang University, Hangzhou, Zhejiang 310027, China

HIGHLIGHTS

- Simulated liquid water transport in turning regions of serpentine gas channels.
- A smooth U-shaped turning region is beneficial to liquid water removal.
- Increased gas stream velocity or surface contact angle assists the process.
- Liquid water tends to accumulate in the sharp right-angled turning region.

ARTICLE INFO

Article history:
Received 27 February 2012
Received in revised form
31 May 2012
Accepted 3 June 2012
Available online 9 June 2012

Keywords:
Lattice Boltzmann simulation
Proton exchange membrane fuel cell
Serpentine gas channel
Two-phase flow
Liquid water transport

ABSTRACT

A two-phase lattice Boltzmann model is employed for direct numerical simulation of liquid water transport in the turning regions of serpentine gas channels in proton exchange membrane (PEM) fuel cells. Two different types of serpentine gas channels with either a smooth U-shaped or a sharp right-angled turning region are examined. Numerical results indicate that a smooth U-shaped turning region is beneficial to liquid water removal in a serpentine gas channel. An increased gas stream velocity or channel surface contact angle can further assist the process. Liquid water tends to accumulate in the sharp right-angled turning region because of the acting direction of the gas shear force. Increased gas stream velocity and surface contact angle are not very helpful for liquid water removal in the right-angled turning region under all the tested conditions. This numerical study is intended to provide improved fundamental understandings of liquid water transport mechanisms in serpentine gas channels of PEM fuel cells.

1. Introduction

Water management is a crucial and challenging issue in research and development of proton exchange membrane (PEM) fuel cells. Many experimental [1–10], macro-scale [11–31] and meso-scale [32–34] numerical studies have been performed to elucidate the underlying physics. Although much progress has been achieved in PEM fuel cell water management, many serious issues still remain, including the numerical model development for liquid water transport in gas channels. Since liquid water transport in gas channels can significantly influence gas supply and cell performance in PEM fuel cells, more fundamental studies are certainly required to better comprehend and optimize this process.

Liquid water dynamic behaviors in gas channels have been experimentally visualized using optically transparent PEM fuel cells [1–3,7]. The physical phenomena of liquid water droplets emerging into, growing, detaching, moving, and interacting inside gas channels were clearly illustrated. Liquid water accumulation and distribution in gas channels under various operation conditions have also been experimentally illuminated using high-resolution neutron imaging [4,9,10] and X-ray radiograph techniques [5,6].

A number of numerical studies have also been conducted to examine liquid water transport dynamics in gas channels of PEM fuel cells. Zhou et al. carried out a series of numerical investigations on liquid water transport behaviors in the cathode gas channel of a PEM fuel cell using the volume-of-fluid (VOF) approach [35–37]. The effects of different channel materials, liquid water properties, and operating conditions on two-phase transport processes have been discussed. Zhu et al. also applied the VOF method to conduct three-dimensional simulation of liquid droplet dynamics in the gas channel of a PEM fuel cell [38]. The effects of air flow velocity, water injection rate, and pore geometry on liquid droplet growth, deformation, and detachment were studied.

* Corresponding author. Tel.: +86 571 87952990.
E-mail address: menghua@zju.edu.cn (H. Meng).

0378-7753/$ – see front matter © 2012 Elsevier B.V. All rights reserved.
http://dx.doi.org/10.1016/j.jpowsour.2012.06.010

Recently, the lattice Boltzmann method has been developed into an efficient and robust numerical scheme for direct simulation of multi-phase fluid flows [39–42]. Different models have been successfully applied for simulating liquid water transport in the porous materials of PEM fuel cells [32–34]. Hao and Cheng applied a two-phase lattice Boltzmann model to simulate liquid droplet dynamics on a hydrophobic surface of a PEM fuel cell gas channel [43]. The formation of a liquid water droplet through a micropore, its subsequent growth and detachment on the channel surface under the air shear force were clearly illustrated. Han et al. further employed the Shan–Chen two-phase lattice Boltzmann model to simulate two liquid droplets development and interaction in the gas channel of a PEM fuel cell [44]. The effects of a number of key influential parameters, including the gas flow velocity, initial droplet distance, different micropore combinations, and the gas diffusion layer (GDL) surface wetting properties on liquid droplets interaction and transport were analyzed.

In this paper, the Shan–Chen two-phase lattice Boltzmann model is employed for direct numerical simulation of liquid water transport in serpentine gas channels of PEM fuel cells, focusing mainly on the liquid droplets transport and interaction in channel turning regions. Two different types of serpentine gas channels with either a smooth U-shaped or a sharp right-angled turning region are examined. The effects of gas stream velocities, channel surface contact angles, droplet sizes, and multiple liquid droplets interactions in the turning region of a serpentine gas channel on liquid water transport behaviors are investigated. Results obtained in this paper are intended to provide deeper fundamental understandings of liquid water transport mechanisms in serpentine gas channels of PEM fuel cells.

2. Model description and validation

In this paper, a lattice Boltzmann model with a single relaxation time collision operator (the so-called LBGK model) and the popular D2Q9 [39] scheme is implemented in a two-dimensional configuration to simulate liquid water transport phenomena in the turning regions of the serpentine gas channels of PEM fuel cells. The Shan–Chen multi-phase model [40–42] is further incorporated for handling two-phase transport phenomena. The lattice Boltzmann method simulates multi-phase fluid flows directly through the evolution of the particle density distribution functions on fixed lattices. The numerical approach proceeds in two steps: collision and streaming. The collision procedure relaxes the density distribution functions on a lattice toward the equilibrium states, while the streaming step moves the particle distributions to the immediate neighboring lattices with specified velocity magnitudes and directions. More details concerning this LBGK model, along with the Shan–Chen two-phase treatment, can be found in our prior publication [44] and the related references cited there.

The two-phase lattice Boltzmann model has been programmed into a computational software package in our group and validated using two test cases concerning the liquid–gas interaction, which leads to phase separation and surface tension, and the liquid–solid interaction, which reveals different wetting characteristics of a solid surface [44]. To provide more confidence on the model and computational software, a numerical simulation has been further conducted for a single liquid water droplet emerging from a micropore and its subsequent development in a hydrophobic channel surface, as shown in Fig. 1. This numerical simulation exactly follows the configuration and conditions used in Ref. [43] (Fig. 8), except that it is conducted in a two-dimension coordinate in the present study. Result in Fig. 1 agrees very well with that in Ref. [43] (Fig. 8). The rigorous model validations conducted in Fig. 1 and our previous publication [44] clearly indicate that the present two-phase lattice Boltzmann model is capable of handling liquid–gas and liquid–solid interactions.

It should be noted that the present LBGK model with the Shan–Chen two-phase treatment solves the single-component two-phase flow problems. Furthermore, because of the existing model limitation, the density ratio between the two phases is only chosen at 10 to ensure numerical accuracy and stability in the present studies. This means that in the two-phase simulations, the liquid phase is water, but the gas phase is dense water vapor. The dense water vapor assumption will affect the gas shear force in the two-phase transport process, rendering it stronger than that in a practical PEM fuel cell gas channel. However, the gas shear force can also be influenced by the flow velocity, whose effect on the liquid droplet movement is investigated in the following parametric studies. Therefore, although with certain numerical limitations, the LBGK model is a good option for directly simulating liquid water transport processes in PEM fuel cells [32–34], especially for qualitative fundamental studies of liquid–gas (surface tension effect) and liquid–solid (contact angle effect) interactions in the PEM fuel cell gas channels.

3. Results and discussion

The two-phase LBGK model briefly described in the last section is employed herein to directly simulate liquid water transport and interaction in the turning regions of serpentine gas channels in PEM fuel cells. Two different types of serpentine gas channels with

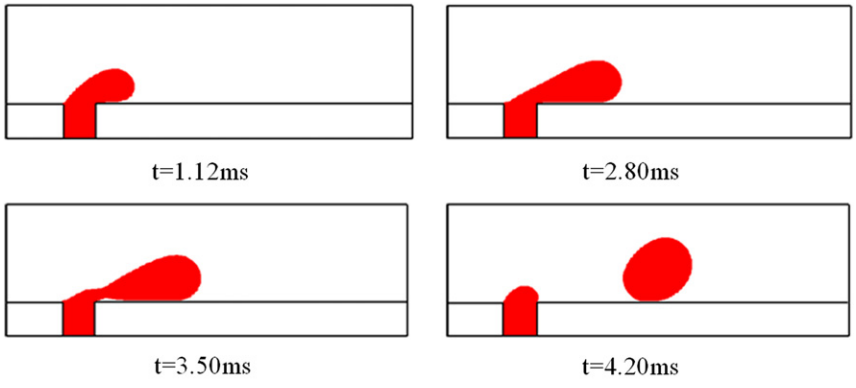

Fig. 1. A single liquid droplet growing into and moving inside the PEM fuel cell gas channel (contact angle 165°).

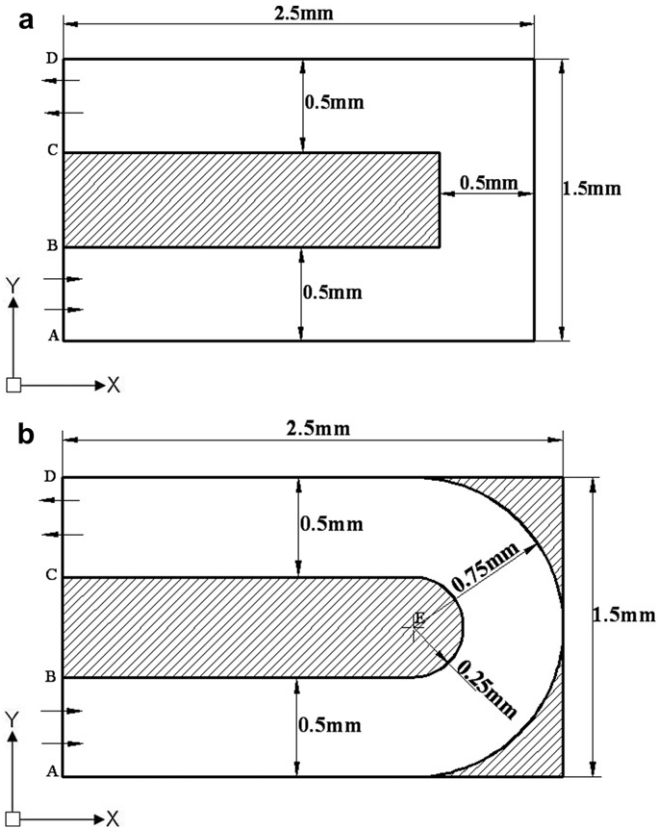

Fig. 2. Geometries of the serpentine gas channels; (a) with a right-angled turning region, and (b) with a U-shaped turning region.

either a smooth U-shaped or a sharp right-angled turning region are examined, as shown in Fig. 2. The shaded regions in Fig. 2 are treated as a solid material in the lattice Boltzmann simulations. It should also be emphasized that in the present two-dimensional simulations, the liquid droplet interaction with GDL has not been considered.

Prior to extensive numerical investigations, a grid independence study is carefully conducted. As shown in Fig. 3, two-set of grid systems with 500*300 and 1000*600 uniform lattices are employed respectively to study the interaction and movement of four liquid water droplets in a U-shaped turning region. No difference is observed in the two set of numerical results. Therefore, a mesh system with 500*300 uniform lattices in the x- and y directions is proved to be sufficient for accurate numerical simulations.

Fig. 4 illustrates the effects of the inlet gas stream velocity on droplet transport behaviors in a smooth U-shaped turning region in a serpentine gas channel. In these studies, the contact angle of the solid channel surface is specified as 90°. A liquid droplet with a diameter of 150 μm is initially placed in the middle of the channel inlet and released with a very small moving speed at 0.1 m s^{-1}. This indicates that the liquid droplet is brought into the turning region by the gas flow. Fig. 4(a) shows a liquid water droplet moving in the channel turning region with an inlet gas stream velocity at 2.5 m s^{-1}. The droplet shows slight deformation close to the solid channel wall, and hits the channel surface at around 0.82 ms. Afterward, it slides smoothly around the U-shaped turning region under the influence of the gas shear force. As the inlet gas velocity is increased to 5.0 m s^{-1}, the liquid droplet behaves similarly in the channel turning region, but moves faster after hitting the channel surface, dragged by a stronger gas share force.

As discussed in the early section, because of the density ratio limitation in the Shan–Chen two-phase LBGK model, the gas phase is a dense water vapor, which could lead to a large gas shear force

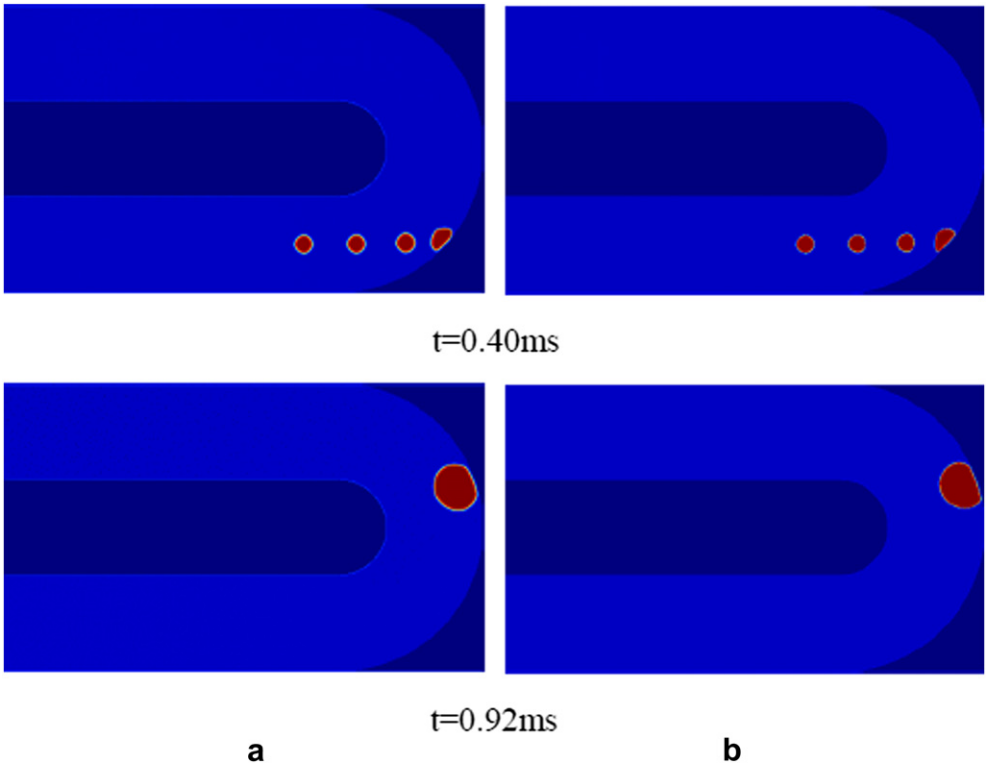

Fig. 3. Results obtained at two different grid resolution conditions; (a) 500*300 lattices and (b) 1000*600 lattices (the gas stream velocity is 2.5 m s^{-1}, the channel surface contact angle is 160°).

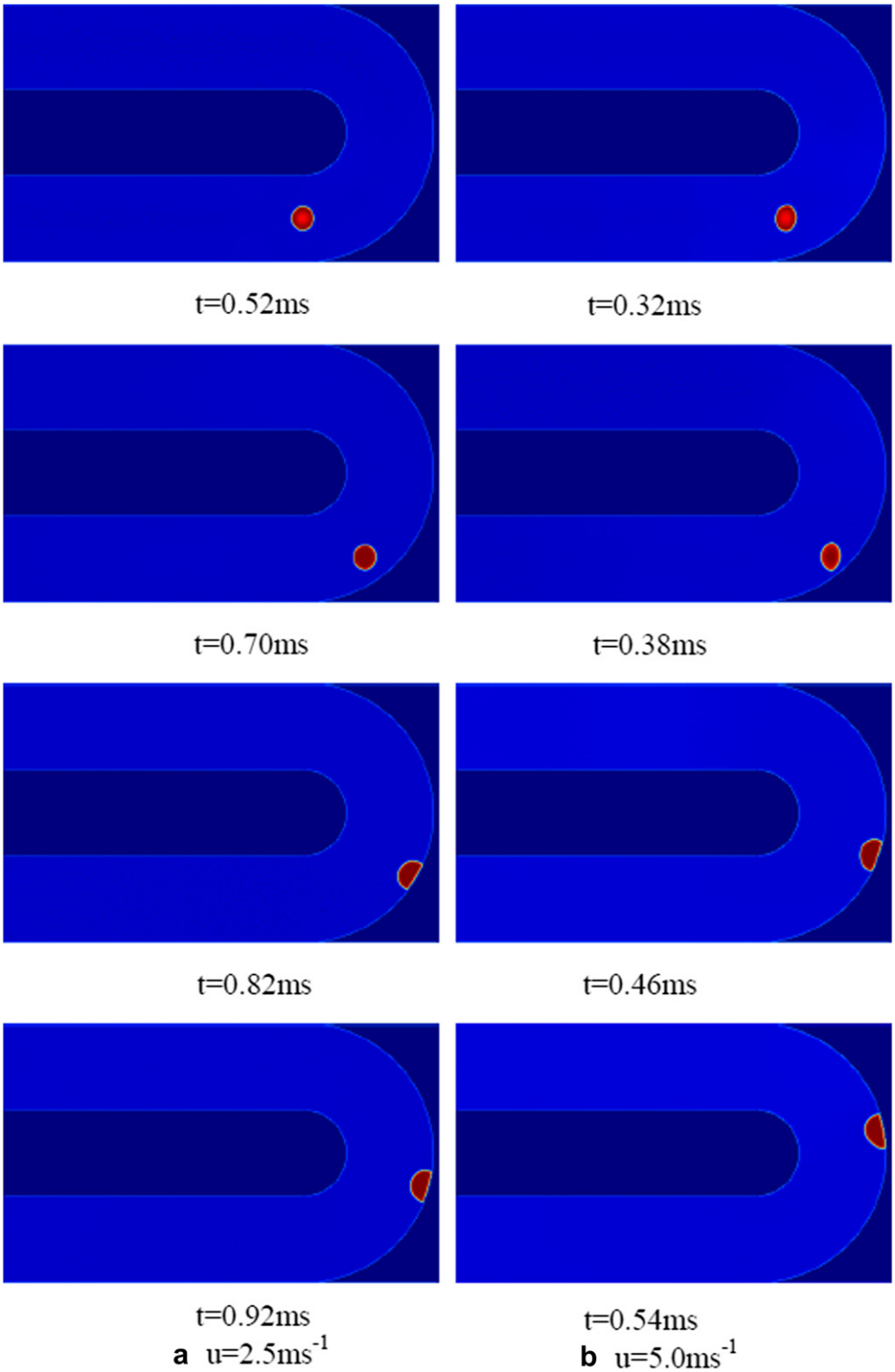

Fig. 4. Effects of the gas stream velocity on liquid droplet transport behaviors in a U-shaped turning region (the channel surface contact angle is 90°).

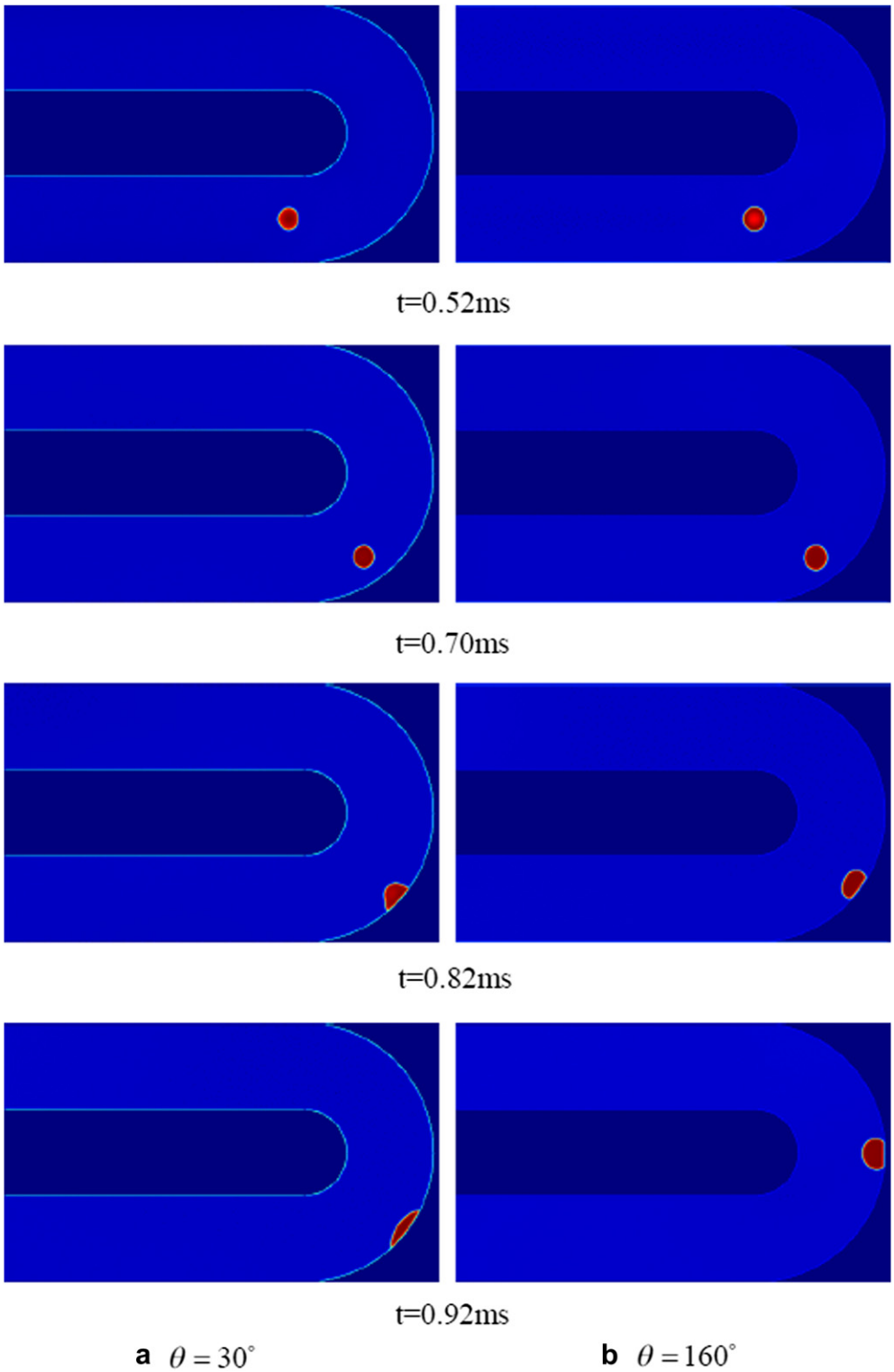

Fig. 5. Effects of the channel surface contact angle on liquid droplet transport behaviors in a U-shaped turning region (the gas stream velocity is 2.5 m s^{-1}).

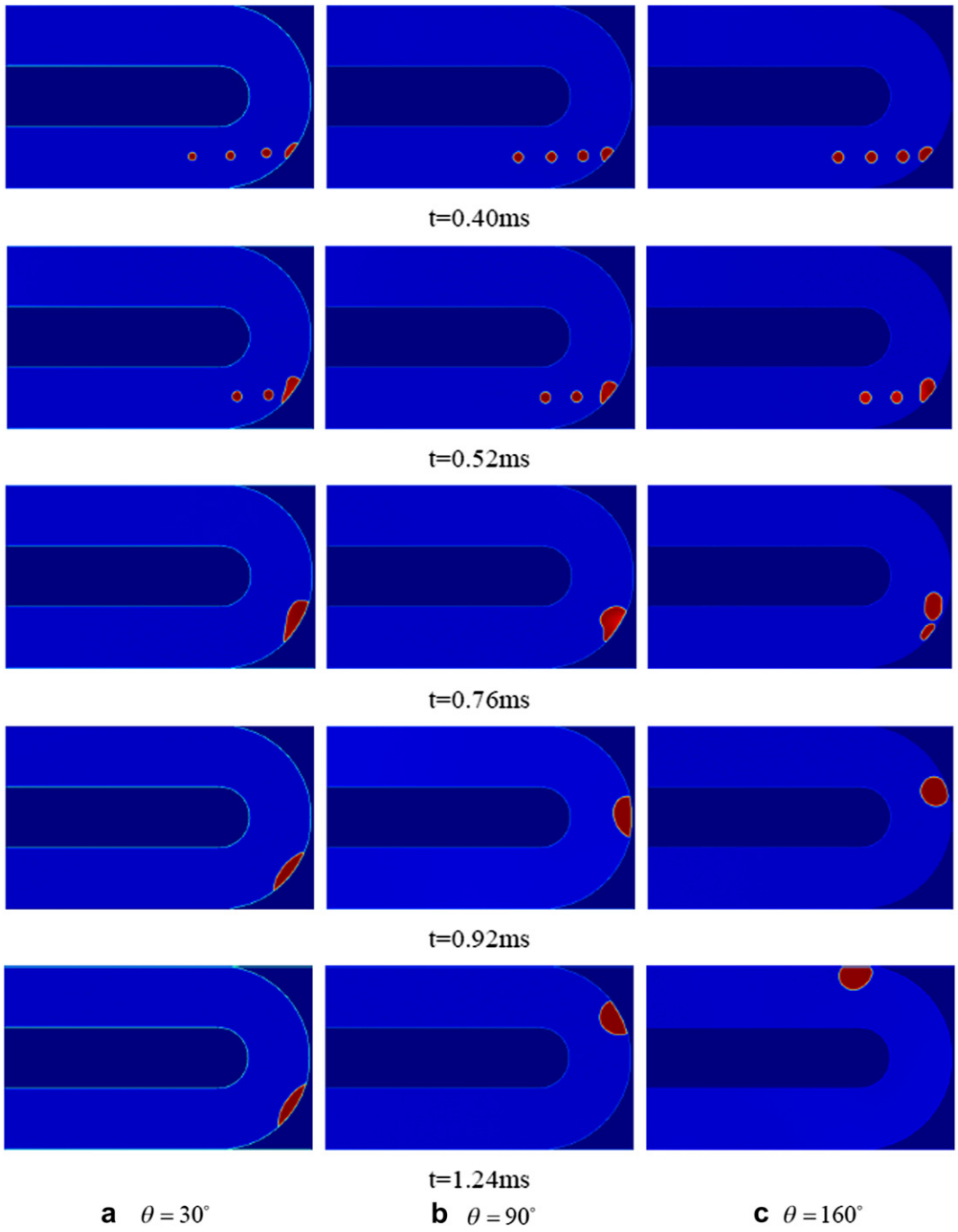

Fig. 6. Multiple droplets interaction and transport in a U-shaped turning region (the gas stream velocity is 2.5 m s^{-1}).

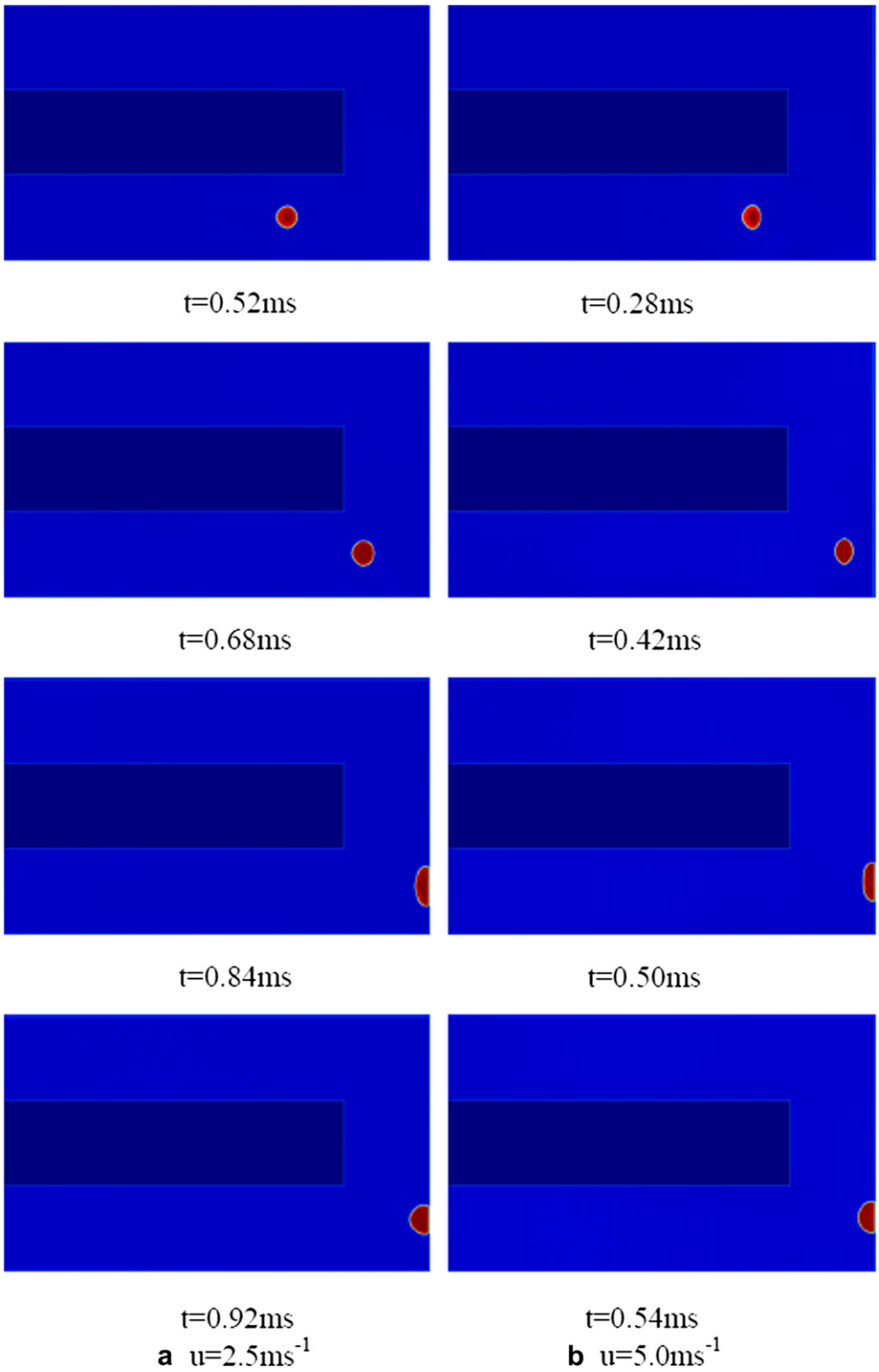

Fig. 7. Effects of the gas stream velocity on liquid droplet transport behaviors in a right-angled turning region (the channel surface contact angle is 90°).

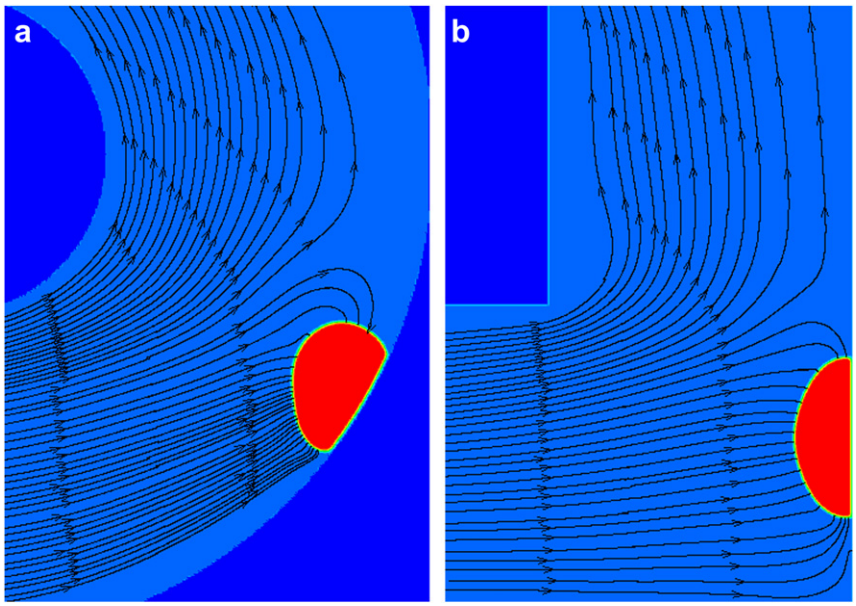

Fig. 8. Gas streamline distributions in (a) the U-shaped and (b) the right-angle turning regions (the gas stream velocity is 2.5 m s^{-1}, the channel surface contact angle is 90°).

acting on the liquid droplet. Therefore, caution is required for direct quantitative extension of the present simulation results to practical PEM fuel cell applications.

The effects of the channel surface wetting property on liquid droplet transport in the U-shaped channel turning region are investigated in Fig. 5. Fig. 5(a) shows that a liquid droplet hits and then spreads on a hydrophilic channel surface with a contact angle at 30°. Its movement is severely hindered afterward. Comparing simulation results in Figs. 5(b) and 4(a), it is found that a liquid droplet moves faster on a hydrophobic channel surface with a larger surface contact angle. Therefore, a more hydrophobic channel surface can promote liquid water removal in the U-shaped turning region in a serpentine gas channel.

Multiple liquid droplets interaction and its subsequent transport behaviors in the U-shaped channel turning region are further examined in Fig. 6. In these cases, four liquid droplets with a same diameter are released from the channel inlet at an equal time interval. With a hydrophilic channel surface at a contact angle of 30°, the four droplets hits the same spot on the channel surface, merges into a large liquid zone, and spreads on the channel surface. Its subsequent movement is hindered, as in the single droplet case. As the surface contact angle is increased to 90°, the four small liquid droplets merges into a large one after hitting the channel wall and then easily moves on the channel surface. Once the channel surface becomes more hydrophobic with a contact angle at 160°, as shown in Fig. 6(c), the first three liquid droplets merges into a large liquid zone on the channel surface and quickly moves away from the hitting spot. The fourth droplet is initially separated from the merged liquid region but can soon catch up with it to form a large liquid droplet and move out of the turning region smoothly. Results in Fig. 6(b) and (c) demonstrate that a large liquid droplet still moves faster on a more hydrophobic channel surface in the smooth U-shaped turning region in a serpentine gas channel.

Fig. 7 shows a liquid water droplet moving in the sharp right-angled turning region in a serpentine gas channel. The contact angle of the solid channel surface is specified as 90°. As illustrated in Fig. 7(a), the liquid droplet released from the channel inlet hits the flat channel surface in the sharp turning region and attaches to it. Further increasing the inlet gas velocity to 5.0 m s^{-1} cannot assist its removal. Therefore, liquid water tends to accumulate in the sharp right-angled turning region in a serpentine gas channel. This phenomenon is caused by the acting direction of the gas shear force, which pushes the liquid droplet toward the channel wall instead of dragging it along the channel surface in the sharp right-angled turning region. It should be further emphasized that given the strong gas shear force resulting from the dense water vapor assumption in the two-phase LBGK model, this conclusion can be safely extended to the practical PEM fuel cell applications.

The gas streamline distributions are provided in Fig. 8(a) and (b), respectively, clearly showing the different gas flow patterns in the U-shaped and right-angled turning regions. The figures are enlarged around the liquid droplet for clear presentation.

The effects of the channel surface wetting property on the liquid droplet transport in the right-angled turning region are investigated in Fig. 9. With different surface contact angles covering both hydrophilic and hydrophobic regimes, the spreading characteristics of the liquid droplet on the channel surface is drastically different, but the liquid droplet remains attached to the channel surface and becomes very difficult to be removed. Results in Figs. 9 and 7(a) clearly indicate that the increased channel surface hydrophobic property cannot assist liquid water removal in the right-angle turning region under the tested conditions.

The effects of the droplet sizes on liquid droplet transport in the right-angled turning region are examined in Fig. 10, with the liquid droplet diameters ranging from 70 to 300 μm. An interesting phenomenon is observed with a large liquid droplet at 300 μm in diameter. As shown in Fig. 10(c), after the large droplet touches the gas channel wall, it is pushed strongly by the gas stream because it blocks a significant portion of the gas flow pathway. Under the action of a strong gas shear force, the droplet is stretched into a thin liquid film and can expand into the corner region.

Fig. 11 elucidates multiple droplets interaction in the sharp right-angled turning region. As in Fig. 6, after four liquid droplets are sequentially released from the channel inlet, they hit the channel surface and subsequently merge into a large liquid zone. Because of the acting direction of the gas shear force, the merged large liquid droplet is very difficult to be removed from the sharp right-angled turning region.

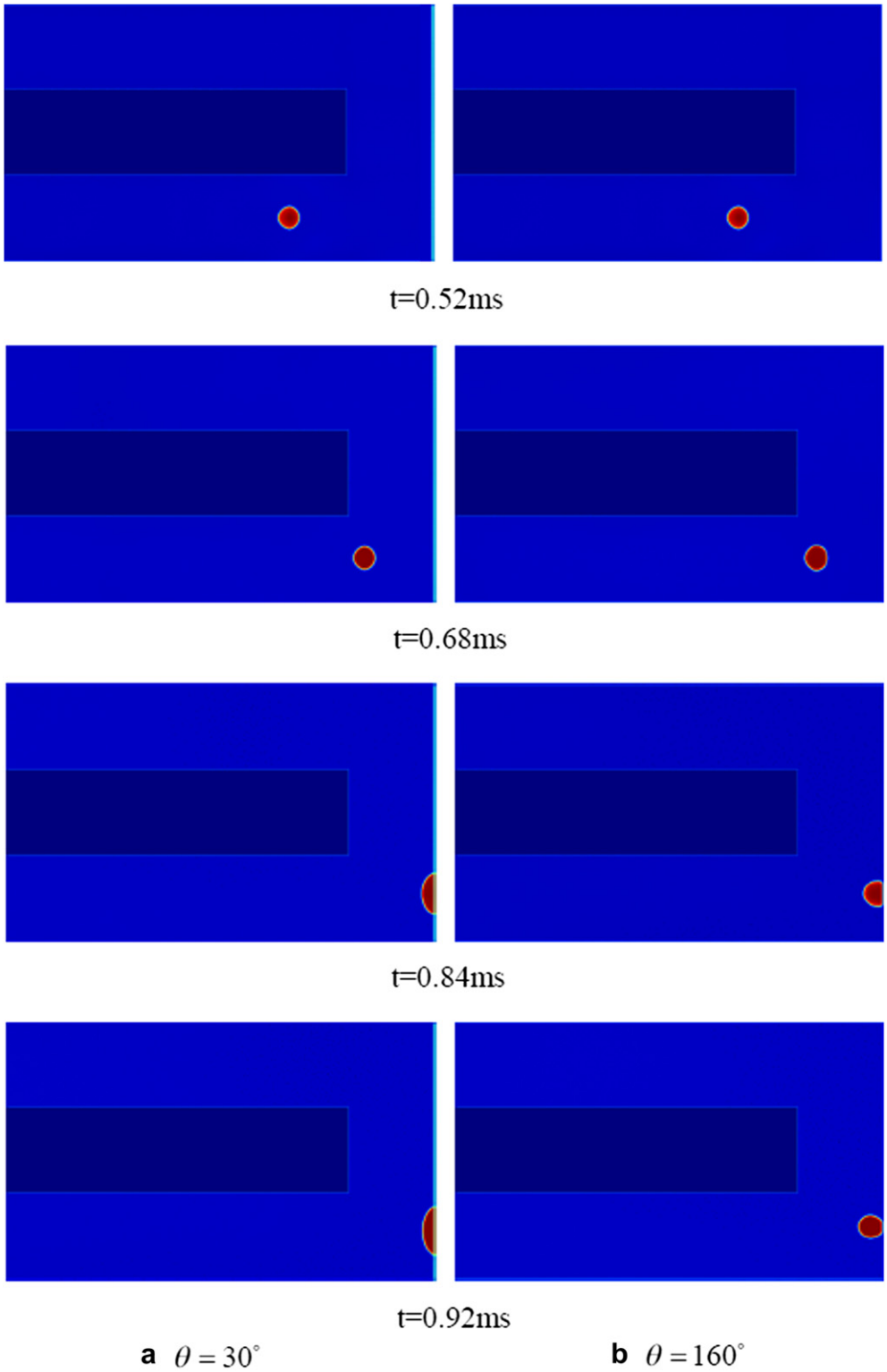

Fig. 9. Effects of the channel surface contact angle on liquid droplet transport behaviors in a right-angled turning region (the gas stream velocity is 2.5 m s^{-1}).

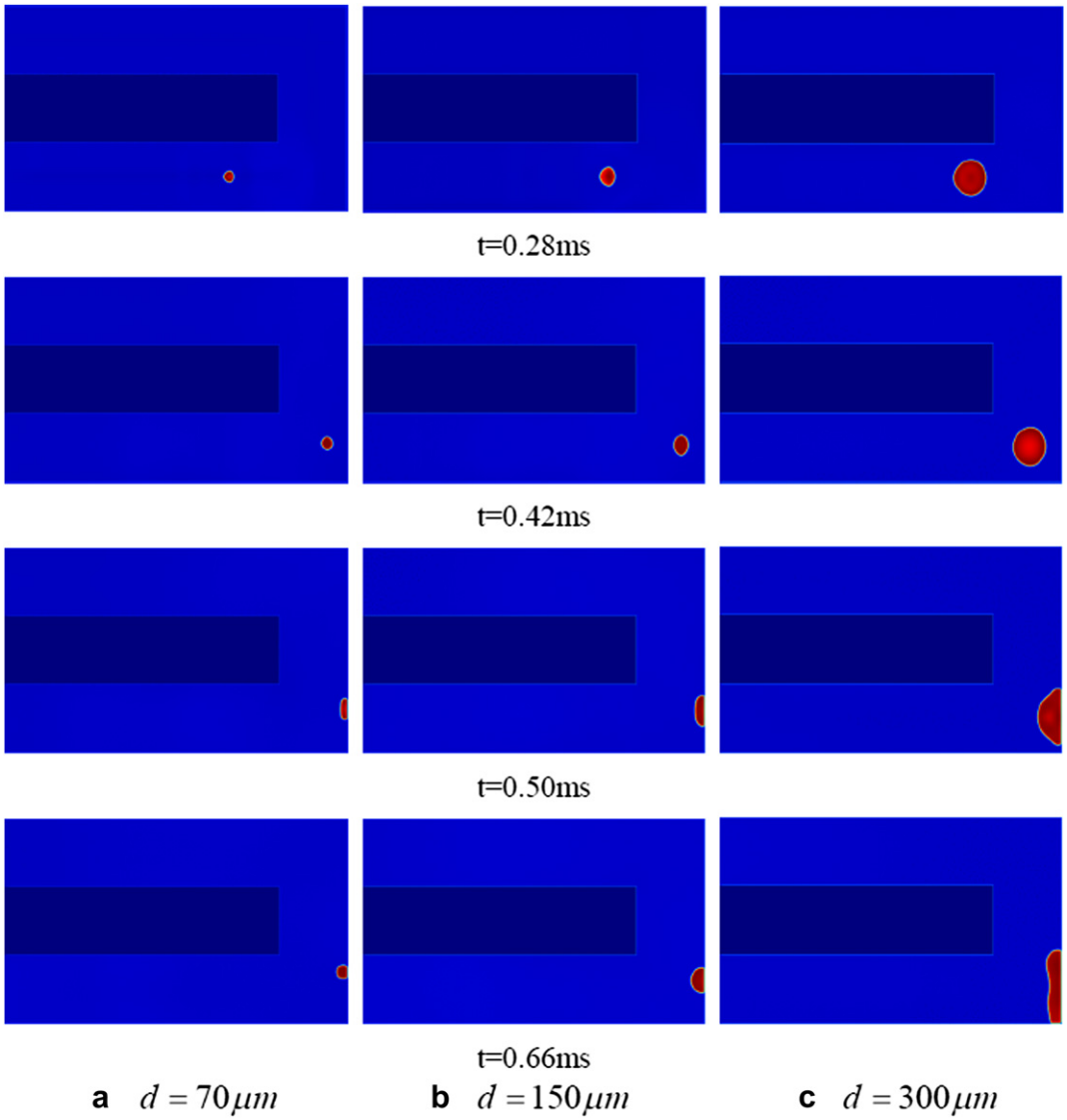

Fig. 10. Effects of the droplet size on liquid droplet transport behaviors in a right-angled turning region (the gas stream velocity is 5.0 m s^{-1}, the channel surface contact angle is 90°).

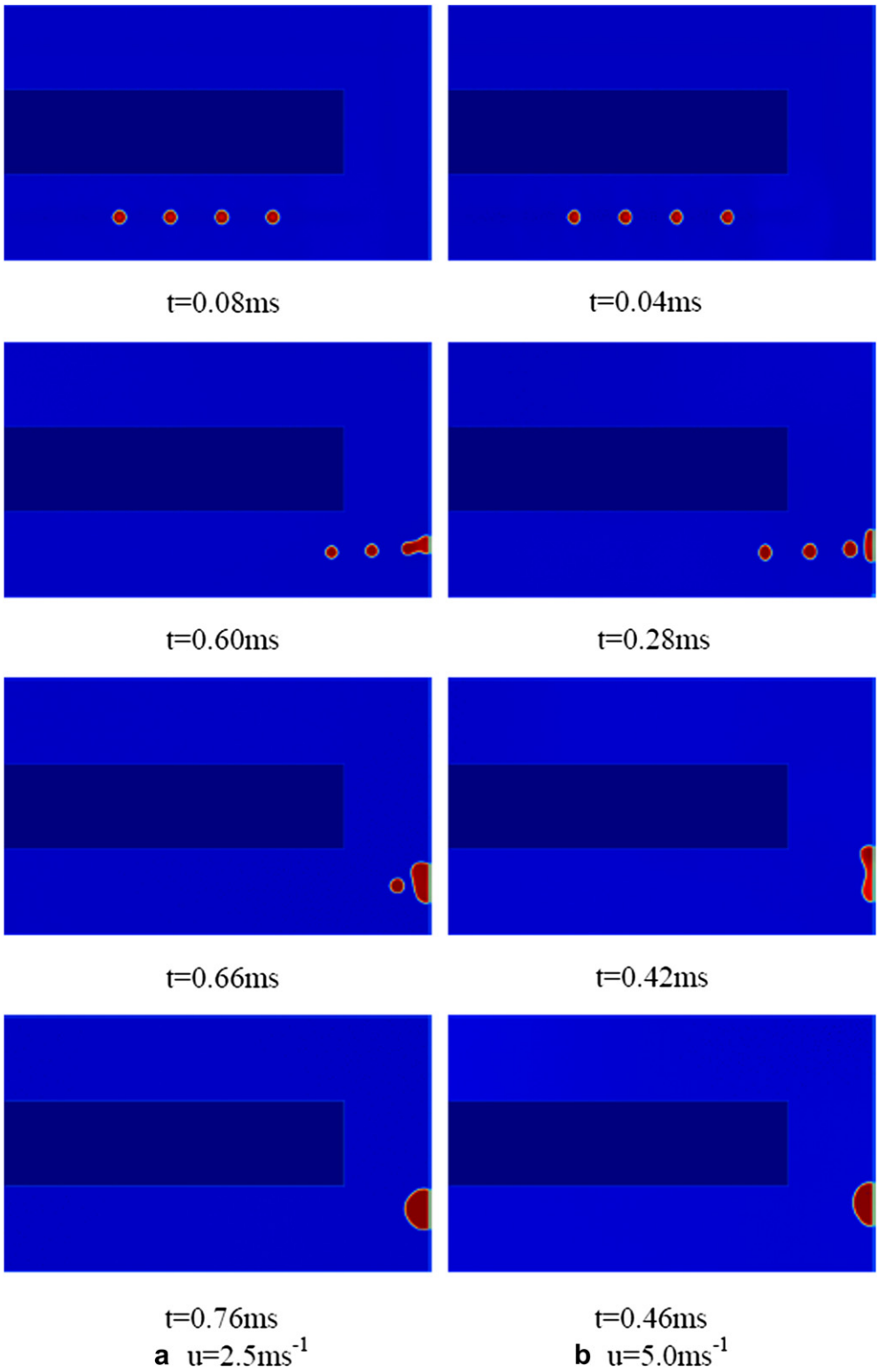

Fig. 11. Multiple droplets interaction and transport in a right-angled turning region (the channel surface contact angle is 90°).

4. Conclusions

The Shan–Chen two-phase lattice Boltzmann model is employed in this paper for direct numerical simulation of liquid water transport in serpentine gas channels of PEM fuel cells, focusing mainly on the fundamental liquid water dynamic behaviors in channel turning regions. Two different types of serpentine gas channels with either a smooth U-shaped or a sharp right-angled turning region are examined. The effects of gas stream velocities, channel surface wetting properties, droplet sizes, and multiple droplets interactions on liquid water transport and distribution in the turning regions are investigated. Numerical results indicate that a smooth U-shaped turning region is beneficial to liquid water removal in a serpentine gas channel. Increased gas stream velocity and channel surface contact angle can further assist liquid water movement in the U-shaped turning region. Liquid water tends to accumulate in the sharp right-angled turning region because of the acting direction of the gas shear force. It is not very helpful for liquid water removal through increasing the gas stream velocity and surface contact angle under the tested conditions in the right-angled turning region in a serpentine gas channel of a PEM fuel cell. It should also be mentioned that because of the density ratio limitation in the model, the dense gas stream may exert a large gas shear force on the liquid droplet. Therefore, caution is required for direct quantitative extension of the present simulation results to practical PEM fuel cell applications.

Acknowledgment

This research work was financially supported by the National Natural Science Foundation of China (No. 10972197).

References

[1] K. Tüber, D. Pócza, C. Hebling, J. Power Sources 124 (2003) 403.
[2] X.G. Yang, F.Y. Zhang, A.L. Lubawy, et al., Electrochem. Solid State Lett. 7 (2004) A408.
[3] F.Y. Zhang, X.G. Yang, C.Y. Wang, J. Electrochem. Soc. 153 (2006) A225.
[4] A. Turhan, K. Heller, J.S. Brenizer, et al., J. Power Sources 160 (2006) 1195.
[5] P.K. Sinha, P. Halleck, C.Y. Wang, Electrochem. Solid State Lett. 9 (2006) A344.
[6] I. Manke, C. Hartinig, M. Grunerbel, et al., Appl. Phys. Lett. 90 (2007) 174105–174113.
[7] D. Spernjak, A.K. Prasad, S.G. Advani, J. Power Sources 170 (2007) 334.
[8] A. Bazylak, D. Sinton, Z.S. Liu, et al., J. Power Sources 163 (2007) 784.
[9] D.S. Hussey, D.L. Jacobson, M. Arif, et al., J. Power Sources 172 (2007) 225.
[10] M.A. Hickner, N.P. Siegel, K.S. Chen, et al., J. Electrochem. Soc. 155 (2008) B427.
[11] W. He, J.S. Yi, T.V. Nguyen, AICHE J. 46 (2000) 2053.
[12] Z.H. Wang, C.Y. Wang, K.S. Chen, J. Power Sources 94 (2001) 40.
[13] L. You, H. Liu, Int. J. Heat Mass Transf. 45 (2002) 2277.
[14] T. Berning, N. Djilali, J. Electrochem. Soc. 150 (2003) A1589.
[15] N.P. Siegel, M.W. Ellis, D.J. Nelson, et al., J. Power Sources 128 (2004) 173.
[16] S. Shimpalee, S. Greenway, D. Spuckler, et al., J. Power Sources 135 (2004) 79.
[17] H. Meng, C.Y. Wang, J. Electrochem. Soc. 152 (2005) A1733.
[18] W.Q. Tao, C.H. Min, X.L. Liu, et al., J. Power Sources 160 (2006) 359.
[19] Y. Wang, C.Y. Wang, J. Electrochem. Soc. 153 (2006) A1193.
[20] H. Ju, G. Luo, C.Y. Wang, J. Electrochem. Soc. 154 (2007) B218.
[21] A.A. Shah, G.S. Kim, W. Gervais, et al., J. Power Sources 160 (2006) 1251.
[22] H. Meng, J. Power Sources 168 (2007) 218.
[23] H. Meng, J. Power Sources 171 (2007) 738.
[24] U. Pasaogullari, P.P. Mukherjee, C.Y. Wang, et al., J. Electrochem. Soc. 154 (2007) B823.
[25] H. Wu, P. Berg, X. Li, J. Power Sources 165 (2007) 232.
[26] K. Jiao, B. Zhou, J. Power Sources 175 (2008) 106.
[27] H. Wu, X. Li, P. Berg, Electrochim. Acta 54 (2009) 6913.
[28] H. Meng, Int. J. Hydrogen Energy 34 (2009) 5488.
[29] H. Meng, Int. J. Hydrogen Energy 35 (2010) 5569.
[30] H. Meng, B. Ruan, Int. J. Energy Res. 35 (2011) 2.
[31] X.-D. Wang, J.-L. Xu, W.-M. Yan, et al., Int. J. Heat Mass Transf. 54 (2011) 2375.
[32] J. Park, X. Li, J. Power Sources 178 (2008) 248.
[33] P.P. Mukherjee, C.Y. Wang, Q. Kang, Electrochim. Acta 54 (2009) 6861.
[34] P.P. Mukherjee, Q. Kang, C.Y. Wang, Energy Environ. Sci. 4 (2011) 346.
[35] P. Quan, B. Zhou, A. Sobiesiak, et al., J. Power Sources 152 (2005) 131.
[36] K. Jiao, B. Zhou, P. Quan, J. Power Sources 157 (2006) 226.
[37] A.D. Le, B. Zhou, H.-R. Shiu, et al., J. Power Sources 195 (2010) 7302.
[38] X. Zhu, P.C. Sui, N. Djilali, J. Power Sources 181 (2008) 101.
[39] Y.H. Qian, D. D'Humières, P. Lallemand, Europhys. Lett. 17 (1992) 479.
[40] X. Shan, H. Chen, Phys. Rev. E 47 (1993) 1815.
[41] X. Shan, H. Chen, Phys. Rev. E 49 (1994) 2941.
[42] H. Huang, Z. Li, S. Liu, et al., Int. J. Numer. Meth. Fluids 61 (2009) 341.
[43] L. Hao, P. Cheng, J. Power Sources 190 (2009) 435.
[44] B. Han, J. Yu, H. Meng, J. Power Sources 202 (2012) 175.